

## Input Estimation Algorithms for Reentry Vehicle Trajectory Estimation

Cheng-Yu Liu

*Lee-Ming Institute of Technology, Taiwan, Republic of China*

and

Huai-Min Wang and Pan-Chio Tuan

*Chung Cheng Institute of Technology, Tao Yuan, Republic of China*

### ABSTRACT

Fast and accurate estimation of trajectory is important in tracking and intercepting reentry vehicles. Validating model is a real challenge associated with the overall trajectory estimation problem. Input estimation technique provides a solution to this challenge. Two input estimation algorithms were introduced based on different assumptions about the input applied to the model. This investigation presents approaches consisting of an extended Kalman filter and two input estimation algorithms to identify the reentry vehicle trajectory in its terminal phase using data from a single radar source. Numerical simulations with data generated from two models demonstrate superior capabilities as measured by accuracy compared to the extended Kalman filter. Evaluation using real flight data provides the consistent results. The comparison between two input estimation algorithms is also presented. The trajectory estimation approaches based on two algorithms are effective in solving the reentry vehicle tracking problem.

Keywords: Reentry vehicle, trajectory estimation, input estimation, extended Kalman filter, reentry vehicle tracking, reentry vehicle interception, reentry vehicle trajectory, validation models, trajectory estimation algorithms, simulation and modelling

### NOMENCLATURE

$a_4, a_5, a_6$	Lateral accelerations	$k$	Starting index of input
$a_4^*, a_5^*, a_6^*$	Model errors	$K_{n+1}$	Kalman gain
$C_b$	Ballistic coefficient	$P_{k+1/k+1-1}$	Covariance matrix of predicted state
$C_{D0}$	Zero-lift drag coefficient	$Q$	Variance of process noise
$g$	Gravity	$R$	Variance of measurement noise
$G_i$	Gain	$s$	Stopping index of input
$H, I$	Identity matrix	$S$	Reference area of the reentry vehicle
		$v_x, v_y, v_z$	Velocity components

Revised 25 February 2005

$V_i$	Variance of the estimated input
$w$	Weight of the reentry vehicle
$x, y, z$	Positions
$X_{k+l}$	State vector with input
$X_{k+l}^*$	State vector with no input
$At$	Sampling period
$\rho$	Air density
$\zeta$	Process noise
$\varepsilon$	Measurement noise
$\xi$	Variance of residual
$\gamma$	Fading factor

## 1. INTRODUCTION

The online estimation of the trajectory of a reentry vehicle (RV) is very important for radar tracking and interception. The main task related to trajectory estimation problems concerns model validation, associated with model error between the mathematical model and the physical system. The model error is typically caused by the simplifying assumptions, manoeuvre and unpredictable external forces during flight, parameter uncertainty, and other sources. To reduce estimation error, all or most quantities in the mathematical model are required to be measurable. Most researchers have addressed post-flight analysis to identify states and key parameters from the flight data measured by sensors such as radar, satellite, and **onboard sensors**<sup>1-4</sup>. **Stepwise** regression, an offline estimation method, is extensively used to determine model structure from flight data measured by radar and inertial sensors'. An online, fast, and accurate trajectory estimation algorithm with data measured by a single radar is needed to solve a **general** reentry vehicle tracking problem. It is more **difficult** and complex than **offline** estimation.

**Chang**<sup>6</sup>, et *al.* defined an online filter for a manoeuvring reentry vehicle based on an augmented Kalman filter. Position, velocity, drag force, and manoeuvre forces yield the augmented state vector and are estimated by an extended Kalman filter. The performance of the proposed Kalman filter,

however, is degraded if a non-maneuvring vehicle is considered. Manohar and **Krishnan**<sup>7</sup> reconstructed a rocket trajectory using differential corrections with measurements that could not be provided by a single radar'. A simple model that includes the unmodelled acceleration input seems to be applicable to estimating trajectory **online** if a recursive determination of input is well defined.

Chen and other researchers introduced input estimation technique to solve tracking **problems**<sup>8-10</sup>. Batched and recursive least-squares method were also successfully used to estimate input in **inverse-heat conduction problems**<sup>11,12</sup>. The proposed input estimations were derived by assuming that the input are constant within the entire operation time of the system. Meanwhile, Lee and Liu assumed the input to be constant over the sampling period to form a recursive algorithm for input **estimation**<sup>13-15</sup>. It provided an accurate estimation in reentry vehicle trajectory estimation and initial leveling in a **strapped-down** inertial navigation system. These two input estimators are built under different hypotheses about the input. This investigation presents the reentry vehicle trajectory estimation methods with these **two input** estimation algorithms and compares their accuracy in terms of trajectory estimation errors by simulations.

This study formulates a reentry vehicle trajectory model with the normal gravity **formula**<sup>16</sup>. Two algorithms for input estimation are derived under two assumptions about input to estimate model errors of the formulated reentry vehicle trajectory model. Trajectory estimation method is then built when the estimated input are substituted into the extended Kalman filter. Simulation results, based on a set of data generated from the reentry vehicle trajectory model with manoeuvring forces, show that the proposed trajectory methods with two input estimators are quite satisfactory. Sets of simulation data from a model with six degrees of freedom (**6-DOFs**) and of real flight data are used to evaluate the performance of the scheme.

## 2. TRAJECTORY MODEL

Consider a flight vehicle in the reentry phase over a flat and nonrotating earth as illustrated in Fig. 1.

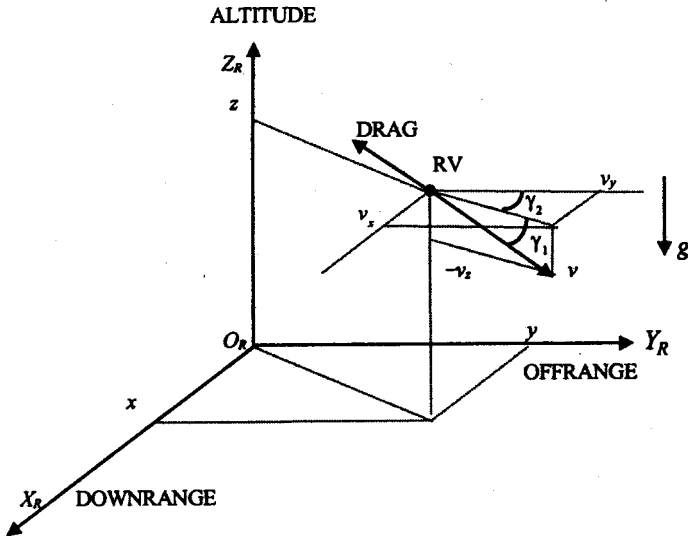


Figure 1. Reentry vehicle flight geometry

Assume the reentry vehicle to be a point mass with constant weight following a ballistic trajectory in which two types of significant forces, drag and gravity, act on the reentry vehicle. The manoeuvring reentry vehicle trajectory model in radar coordinate  $(O_R, X_R, Y_R, Z_R)$  centred at the radar site, can be expressed as<sup>17</sup>

$$\dot{v}_x = -\frac{\rho v^2}{2C_b} g \cos \gamma_1 \sin \gamma_2 + a_4 \quad (1)$$

$$\dot{v}_y = -\frac{\rho v^2}{2C_b} g \cos \gamma_1 \cos \gamma_2 + a_5 \quad (2)$$

$$\dot{v}_z = \frac{\rho v^2}{2C_b} g \sin \gamma_1 - g + a_6 \quad (3)$$

where

$$C_b = \frac{W}{S C_{D0}}$$

$$\gamma_1 = \tan^{-1}\left(\frac{v_z}{\sqrt{v_x^2 + v_y^2}}\right) \quad \gamma_2 = \tan^{-1}\left(\frac{v_x}{v_y}\right)$$

The normal gravity model  $g$ , which is a function of altitude, is employed.

Equations (1) to (3) are formulated with certain assumptions such as point mass and constant weight of the reentry vehicle. Extra acceleration is considered to describe the model error induced by violation of assumptions, unpredictable and unexpected forces during flight, parameters uncertainty, and other sources. Let input of the model be

$$u_i = a_i + a_i^* \quad i = 4, 5, 6 \quad (4)$$

The model can be rewritten as

$$\dot{v}_x = -\frac{\rho v^2}{2C_b} g \cos \gamma_1 \sin \gamma_2 + u_4 \quad (5)$$

$$\dot{v}_y = -\frac{\rho v^2}{2C_b} g \cos \gamma_1 \cos \gamma_2 + u_5 \quad (6)$$

$$\dot{v}_z = \frac{\rho v^2}{2C_b} g \sin \gamma_1 - g + u_6 \quad (7)$$

Let the state vector be

$$X = [x_1 \ x_2 \ x_3 \ x_4 \ x_5 \ x_6]^T = [x \ y \ z \ v_x \ v_y \ v_z]^T \quad (8)$$

The nonlinear state equation can be written as

$$\dot{X} = F(X) + \varphi u + I_{6 \times 6} \zeta \quad (9)$$

where

$$F(X) = \begin{bmatrix} x_4 \\ x_5 \\ x_6 \\ -\frac{\rho}{2C_b} (x_4^2 + x_5^2 + x_6^2) g \cos \gamma_1 \sin \gamma_2 \\ -\frac{\rho}{2C_b} (x_4^2 + x_5^2 + x_6^2) g \cos \gamma_1 \cos \gamma_2 \\ \frac{\rho}{2C_b} (x_4^2 + x_5^2 + x_6^2) g \sin \gamma_1 - g \end{bmatrix}$$

$$\phi = \begin{bmatrix} 0_{3 \times 3} & 0_{3 \times 3} \\ 0_{3 \times 3} & I_{3 \times 3} \end{bmatrix}$$

$$u = [0 \ 0 \ 0 \ u_4 \ u_5 \ u_6]^T$$

A precision digital phase array radar is considered in the system for detecting the reentry vehicle. The detected target's position is transferred into Cartesian frame first and filtered as position, velocity, and acceleration by an  $\alpha$ - $\beta$  filter. Since the filtered acceleration has less accuracy, the filtered position and velocity are usually taken as the main measurements of the radar. The measurement equation ignoring the process inside radar is then formulated as

$$Z = HX + \varepsilon \tag{10}$$

in which noise vector  $\varepsilon$  is assumed to be a set of independent random variables with diagonal covariance matrix  $R$ . Equations (9) and (10) form the dynamic equations for the vehicle during reentry.

The predicted and updated state vectors of the extended Kalman filter (EKF) with input vector  $u_n$  from  $t = n\Delta t$  to  $t = (n+1)\Delta t$ ,  $n = 0, 1, 2, \dots$ , are given<sup>18</sup> by

$$\hat{X}_{n+1/n} = \phi_n \hat{X}_{n/n} + \phi u_n \tag{11}$$

$$\hat{X}_{n+1/n+1} = \hat{X}_{n+1/n} + K_{n+1}(Z_{n+1} - H\hat{X}_{n+1/n}) \tag{12}$$

where

$$\phi_n = I_{6 \times 6} + \left. \frac{\partial F(X)}{\partial X} \right|_{X=\hat{X}_{n/n}} \Delta t$$

### 3. RECURSIVE INPUT ESTIMATION

The extended Kalman filter will typically converge with long time propagation if  $u_n$  is omitted in Eqn (11). However, a long convergence time is unacceptable for online requirement. An algorithm must be developed to estimate the input acceleration and achieve a rapid and accurate trajectory estimation that yields some desired level of accuracy.

Let  $\bar{X}_{n+1/n}$  and  $\bar{X}_{n+1/n+1}$  denote the predicted and updated states, respectively, for the EKF with no input at  $t = (n+1)\Delta t$ . For simplicity, denote  $\hat{X}_{n+1} = \hat{X}_{n+1/n+1}$ ,  $\bar{X}_{n+1} = \bar{X}_{n+1/n+1}$ , and let  $M_{n+1} = (I - K_{n+1}H)\phi_n$ ,  $N_{n+1} = (I - K_{n+1}H)\phi$ . The updated state can be organised as

$$\bar{X}_{n+l} = \left( \prod_{i=n+1}^{n+l} M_i \right) \bar{X}_n + \sum_{j=1}^{l-1} \left( \prod_{i=1+j}^{l-1} M_{n+i} \right) K_{n+j} Z_{n+j} + K_{n+l} Z_{n+l} \tag{13}$$

$l = 0, 1, 2, \dots$

Assume that an input is applied during  $k\Delta t \leq t \leq (k+s)\Delta t$ ,

$$u = \begin{cases} 0 & t < k\Delta t, t > (k+s)\Delta t \quad k, s > 0 \\ u_{k+l} & k\Delta t \leq t \leq (k+s)\Delta t \quad l = 0, 1, 2, \dots, s \end{cases} \tag{14}$$

The updated state vector in the EKF formation with input is given by

$$\begin{aligned} \hat{X}_{k+l} &= \left( \prod_{i=k+1}^{k+l} M_i \right) \hat{X}_k \\ &+ \sum_{j=1}^{l-1} \left( \prod_{i=1+j}^{l-1} M_{k+i} \right) (K_{k+j} Z_{k+j} + N_{k+j} u_{k+j-1}) \\ &+ K_{k+l} Z_{k+l} + N_{k+l} u_{k+l-1} \end{aligned} \tag{15}$$

with  $\hat{X}_k = \bar{X}_k$ . Let the difference between these two formations be

$$\Delta X_{k+l} = \hat{X}_{k+l} - \bar{X}_{k+l} \tag{16}$$

Define the residuals for the EKF formation without and with input to be

$$\bar{Z}_{k+l} = Z_{k+l} - H\bar{X}_{k+l}; \quad \hat{Z}_{k+l} = Z_{k+l} - H\hat{X}_{k+l}$$

#### 3.1 Algorithm 1

Suppose  $u_{k+l}$ ,  $l = 1, 2, \dots, s$  to be constant vector within  $k\Delta t \leq t \leq (k+s)\Delta t$ . Substituting  $\hat{X}_{k+l}$  and  $\bar{X}_{k+l}$  into Eqn (16), one has:

$$\Delta X_{k+l} = \begin{cases} (I - K_{k+l}H)(\Phi_{k+l}\Delta X_{k+l-1} + \Phi u_{k+l-1}) & k\Delta t \leq t \leq (k+s)\Delta t \\ 0 & \text{otherwise} \end{cases} \quad (17)$$

Since the input are all constant, let

$$\Delta X_{k+l} = A_{k+l} \Phi u_{k+l-1} \quad (18)$$

where  $A_{k+l}$  is a constant matrix at  $t = (k+l)\Delta t$  and  $A_k = 0$ .

Substituting Eqn (18) into Eqn (17), it yields:

$$A_{k+l} = \begin{cases} (I - K_{k+l}H)(\Phi_{k+l}A_{k+l-1} + I) & k\Delta t \leq t \leq (k+s)\Delta t \\ 0 & \text{otherwise} \end{cases} \quad (19)$$

The regression equation can then be written as

$$\bar{Z}_{k+l} = B_{k+l} u_{k+l-1} + \hat{Z}_{k+l} \quad (20)$$

where

$$B_{k+l} = HA_{k+l}\Phi$$

The recursive least-squares input estimator, named algorithm 1, can be expressed<sup>11,12</sup> by

$$\hat{u}_{k+l-1} = \hat{u}_{k+l-2} + G_{k+l}(\bar{Z}_{k+l} - B_{k+l}\hat{u}_{k+l-2}) \quad (21)$$

where

$$G_{k+l} = \gamma^{-1}V_{k+l-1}B_{k+l} \left[ B_{k+l}\gamma^{-1}V_{k+l-1}B_{k+l}^T + \xi \right]^{-1}$$

$$V_{k+l-1} = [I - G_{k+l-1}B_{k+l-1}]V_{k+l-2}$$

$$\xi = R + HP_{k+l+1/k+l}H^T$$

From the regression equation,  $\bar{Z}_{k+l}$  excites the input estimation mechanism.  $\bar{Z}_{k+l}$  can be rewritten as

$$\bar{Z}_{k+l} = (Z_{k+l} - HX_{k+l}^*) + H(X_{k+l}^* - \bar{X}_{k+l})$$

The terms of  $Z_{k+l} - HX_{k+l}^*$  and  $X_{k+l}^* - \bar{X}_{k+l}$  represent the estimation errors induced by the input and the **EKF** with no input at  $t = (k+l)\Delta t$ , respectively. It means that the estimated input contains not only input but also state estimation errors consisting of truncation error, uncertainty of initial values, measurement noise, and so on. Although an actual input cannot be estimated, a precise trajectory estimation is reached. In addition, both batched and recursive input estimators are available for algorithm 1.

### 3.2 Algorithm 2

Assume  $u_{k+l}$  to be a constant vector over the sampling period  $\Delta t$ . The difference induced by the abrupt input,  $\Delta X_{k+l}$ , can be written as

$$\Delta X_{k+l} = M_{k+l} \Delta X_{k+l-1} + N_{k+l} u_{k+l-1}$$

The residual is then expressed by

$$\bar{Z}_{k+l} = HM_{k+l} \Delta X_{k+l-1} + HN_{k+l} u_{k+l-1} + \hat{Z}_{k+l}$$

It leads to the regression equation

$$Y_{k+l} = \Phi_{k+l} u_{k+l-1} + \hat{Z}_{k+l} \quad (22)$$

where  $Y_{k+l}$  means the pseudo measurement vector,

$$Y_{k+l} = \bar{Z}_{k+l} - HM_{k+l} \Delta X_{k+l-1}$$

$$\Phi_{k+l} = HN_{k+l}$$

Therefore, algorithm 2 for input estimation<sup>15</sup> is given by

$$\hat{u}_{k+l-1} = \hat{u}_{k+l-2} + G_{k+l}(\hat{Y}_{k+l} - \Phi_{k+l}\hat{u}_{k+l-2}) \quad (23)$$

where

$$\hat{Y}_{k+l} = \bar{Z}_{k+l} - HM_{k+l} \Delta \hat{X}_{k+l-1}$$

$$\Delta \hat{X}_{k+l-1} = M_{k+l-1} \Delta \hat{X}_{k+l-2} + N_{k+l} \hat{u}_{k+l-2}$$

$$G_{k+l} = V_{k+l-1} \Phi_{k+l} \xi^{-1}$$

$$V_{k+l-1} = V_{k+l-2}$$

$$- V_{k+l-2} \Phi_{k+l}^T [\Phi_{k+l} V_{k+l-2} \Phi_{k+l}^T + \xi]^{-1} \Phi_{k+l} V_{k+l-2}$$

where  $\xi$  is the same as algorithm 1.

The pseudo measurement vector  $Y_{k+l}$  can be rewritten as

$$\hat{Y}_{k+l} = [(Z_{k+l} - HX_{k+l}^*) + HM_{k+l}(\hat{X}_{k+l-1} - \bar{X}_{k+l-1})] + H(X_{k+l}^* - \bar{X}_{k+l})$$

The term,  $\hat{X}_{k+l-1} - \bar{X}_{k+l-1}$ , represents the difference between the EKF with no input and with input at the previous time interval. It is an extra term as comparing to algorithm 1 that leads algorithm 2 to be more accurate than algorithm 1. However, algorithm 2 is more complex and recursive input estimator is its only choice.

In Eqn (14),  $k$  and  $s$  represent the starting and stopping indices of the system input, respectively, and can be determined by testing. The test for detection of input for two algorithms is defined as<sup>15</sup>

$$\left| \frac{\hat{u}_i}{\sqrt{V_{ii}}} \right| > t_{st} \text{ existence of } u_i \text{ for } i=4,5,6 \quad (24)$$

otherwise  $u_i$  is absent where  $V_{ii}$  denotes the  $ii^{\text{th}}$  element of  $V$  and  $[-t_{st}, t_{st}]$  is the confidence interval. Suppose the test defined in Eqn (24) to be normally distributed, then, the value oft., can be determined by inspecting the cumulative normal distribution table for a preset confidence coefficient  $\alpha$ .

#### 4. TRAJECTORY ESTIMATION

Once the input is estimated, the EKF is corrected by the estimated input at the same time. By incorporating the online input estimator into the EKF, the predicted and updated states at time interval  $k\Delta t \leq t \leq (k + s)\Delta t$  are:

$$\hat{X}_{k+l/k+l-1}^v = \Phi_{k+l-1} \hat{X}_{k+l-1/k+l-1}^v + \Phi \hat{u}_{k+l-1} \quad (25)$$

$$\hat{X}_{k+l/k+l}^v = \hat{X}_{k+l/k+l-1}^v + K_{k+l}^v (Z_{k+l} - H\hat{X}_{k+l/k+l-1}^v) \quad (26)$$

The Kalman gain becomes:

$$K_{k+l}^v = P_{k+l/k+l-1}^v H^T (HP_{k+l/k+l-1}^v H^T + R)^{-1} \quad (27)$$

with the covariance matrices of the adaptive filter at  $k\Delta t \leq t \leq (k + s)\Delta t$  being

$$P_{k+l/k+l-1}^v = P_{k+l/k+l-1} + \Phi_{k+l-1} L_{k+l} \Phi_{k+l-1}^T + \Phi V_{k+l-1} \Phi^T = P_{k+l/k+l-1} + P'_{k+l/k+l-1} \quad (28)$$

$$P_{k+l/k+l}^v = (I - K_{k+l}^v H) P_{k+l/k+l-1}^v \quad (29)$$

where

$$P'_{k+l/k+l-1} = \Phi_{k+l-1} L_{k+l} \Phi_{k+l-1}^T + \Phi V_{k+l-1} \Phi^T$$

$$L_{k+l} = 0 \quad L_{k+2} = N_{k+2} V_k N_{k+2}^T$$

$$L_{k+l} = \sum_{j=1}^{l-1} \left( \prod_{i=1+j}^l M_{k+i-1} \right) N_{k+j} V_{k+j-1} N_{k+j}^T \left( \prod_{i=1+j}^l M_{k+i-1}^T \right)$$

$$= M_{k+l-1} L_{k+l-1} M_{k+l-1}^T$$

$P'_{k+l/k+l-1}$  denotes the increment in covariance introduced by  $\hat{u}_i$ ,  $i = k, k + 1, \dots, k + l-1$ . For time beyond the interval  $k\Delta t \leq t \leq (k + s)\Delta t$ , state estimation can also be based upon the original EKF. It is noted that the initial states and covariance matrices at  $t > (k + s)\Delta t$  are reinitiated by  $\hat{X}_{k+s/k+s}^v$  and  $P_{k+s/k+s}^v$ . Figure 2 schematically depicts the proposed method which consists of the EKF and algorithm 1 or algorithm 2. The detailed steps of the proposed method are given in Appendix 1.

#### 5. SIMULATION ANALYSIS

This section evaluates the performance of the trajectory estimation methods with two algorithms in terms of trajectory estimation errors by simulations.

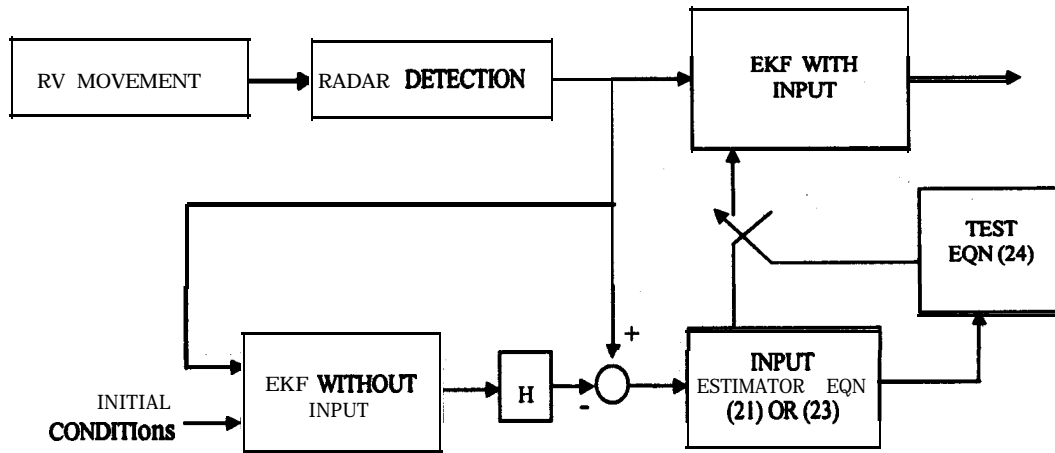


Figure 2. Mechanism of the proposed filter scheme

Two cases of simulation, whose data are generated from the two different models, have been presented.

#### Case 1

A typical manoeuvring trajectory is generated from Eqns (1)-(3) with  $C_b = 2524 \text{ kg/m}^2$  and lateral accelerations,  $a_x = 5 \text{ g}$ ,  $a_y = 5 \text{ g}$ , and  $a_z = 15 \text{ g}$  during  $5 \text{ s} \leq t \leq 10 \text{ s}$ ,  $12 \text{ s} \leq t \leq 16 \text{ s}$ , and  $15 \text{ s} \leq t \leq 20 \text{ s}$ , respectively. Figures 3 and 4 demonstrate the measured trajectory with normally distributed measurement noise.

During estimation,  $C_b = 5048 \text{ kg/m}^2$  is assigned to increase the model error for showing the necessity

of input estimation. Let  $a = 0.95$ ,  $R = 0.03 \text{ I}$ ,  $Q = 0.03 \text{ I}$ , and  $A_t = 0.05 \text{ s}$ . Initial of  $V$  is taken as  $20 \text{ I}$ . Figures 5 and 6 illustrate the estimation errors in position and velocity, respectively, using the EKF with no input. Figure 7 shows the standard deviation for position and velocity. Large estimation errors along downrange, offrange, and altitude axes are unacceptable for tracking and interception. The standard deviations of the estimated state are all bounded and small. Figures 8 and 9 display the estimation errors in position and velocity generated by the EKF with two input estimation algorithms. Obviously, it is much less than by the EKF with no input and shows that the EKF with input estimator

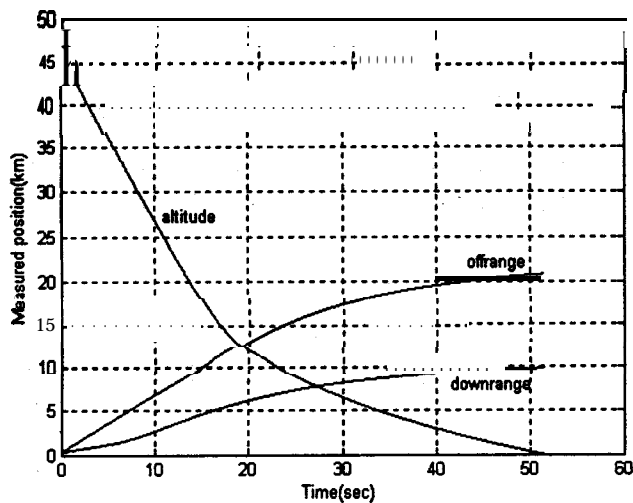


Figure 3. Measured position for Case 1

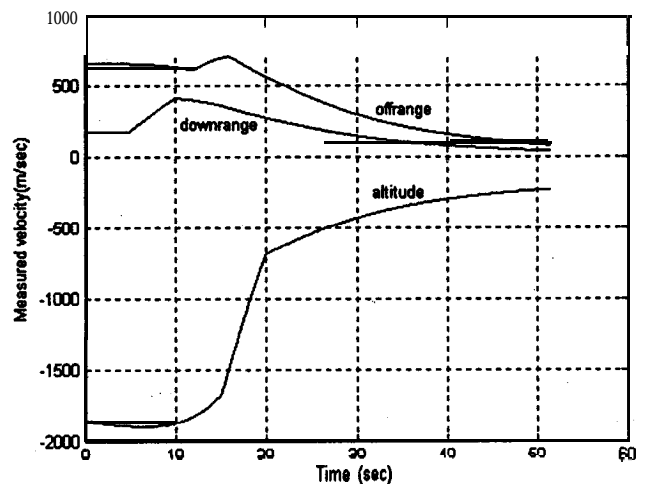


Figure 4. Measured velocity for Case 1

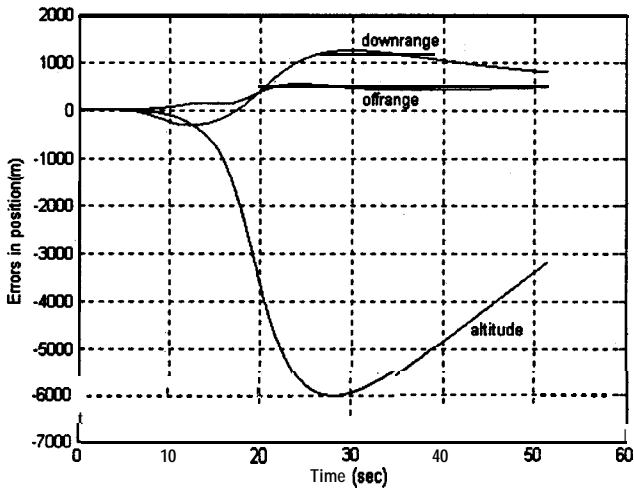


Figure 5. Position estimation error using EKF without input estimation for *Case 1*.

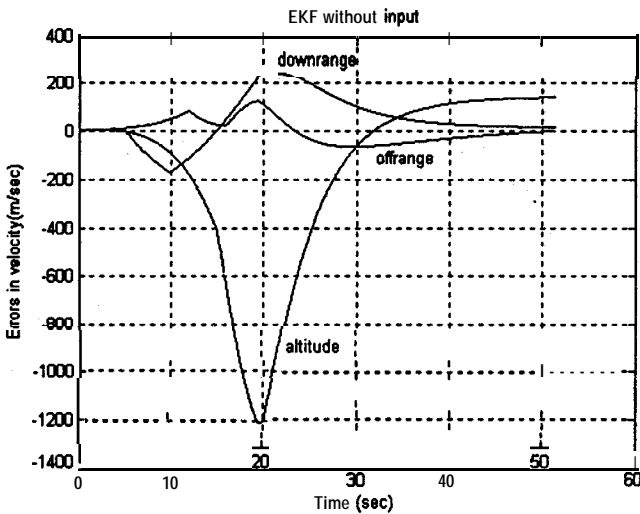


Figure 6. Velocity estimation error using EKF without input estimation for *Case 1*.

is much better than the original EKF. Input estimation indeed plays an important role. Figures 10 and 11 compare the standard deviation of the estimated position and velocity, respectively, for two input algorithms that are small and bounded too. It represents that the estimated trajectories using these three methods are deviated from their own in a small region with certain probabilities.

Comparing these two algorithms, the estimation errors induced by the EKF with algorithm 2 are half of errors provide by the EKF with algorithm 1. It is reasonable since the assumption of the algorithm 2

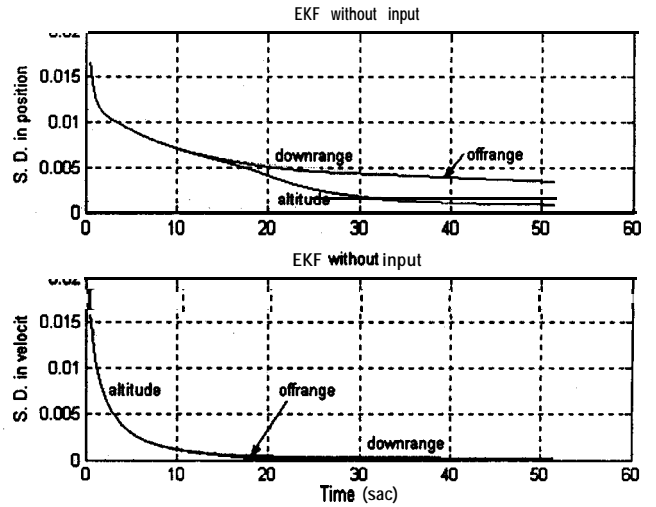


Figure 7. Standard deviation of the estimated states for *Case 1*.

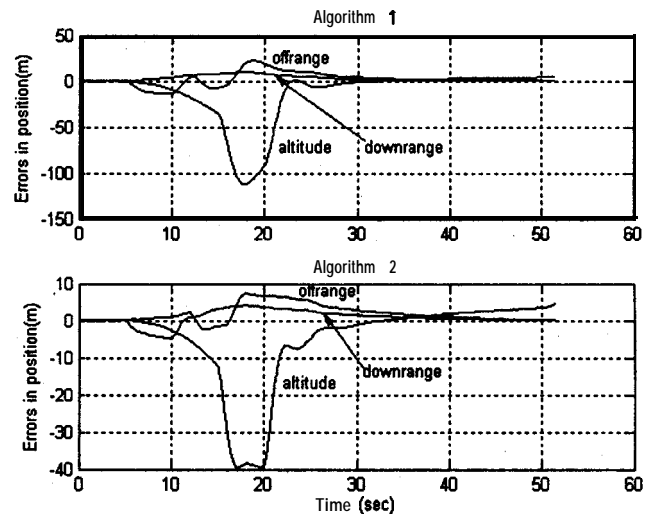


Figure 8. Position estimation error using EKF with input estimation for *Case 1*.

about the input is more close to the real. Algorithm 2 is more accurate than algorithm 1 but more complicated. Selection of algorithm 1 or algorithm 2 depends on what the main concern is.

### Case 2

A set of data, generated from a 6-DOFs model, was employed to demonstrate how the proposed methods process the model error. The 6-DOFs model of a flying vehicle is a set of equations of motion including both translational and rotational motion. It is more detailed than the 3-D model indicated in Eqns (1)-(3).



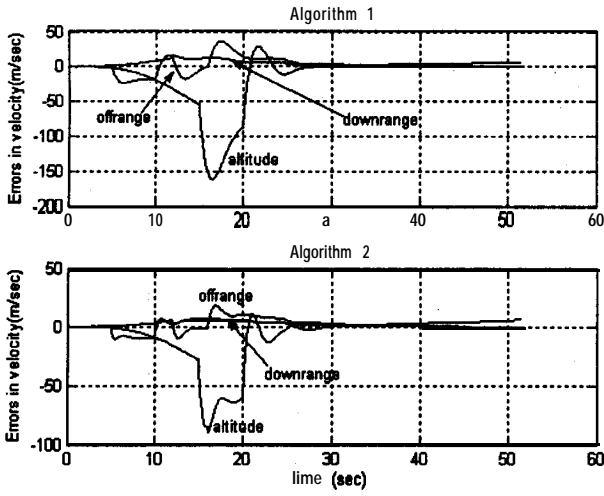


Figure 9. Velocity estimation error using EKF with input estimation for *Case 1*.

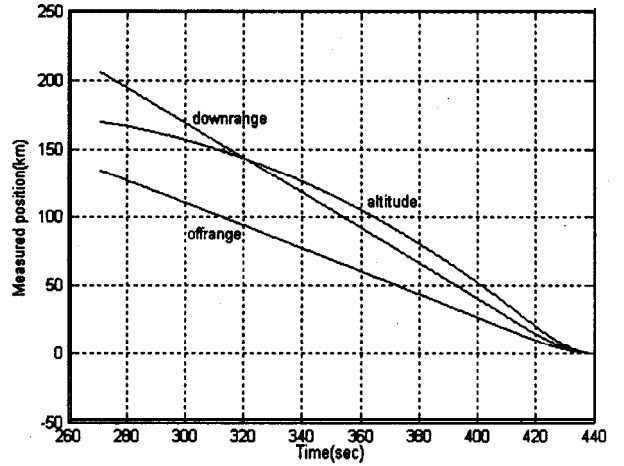


Figure 12. Measured position for *Case 2*

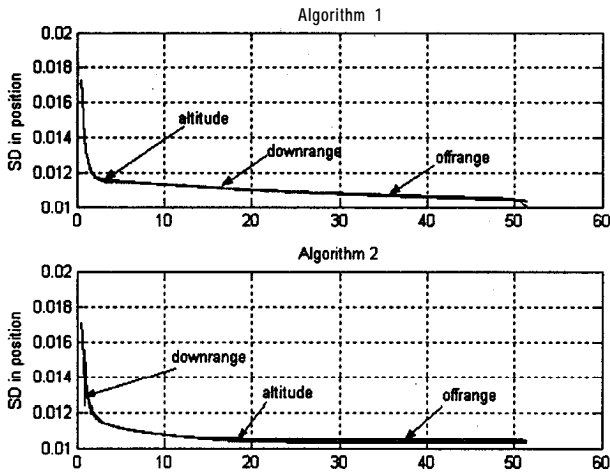


Figure 10. Standard deviation of the estimated position for *Case 1*.

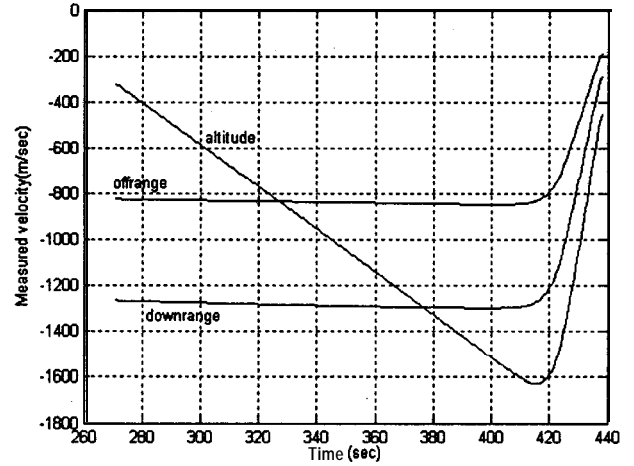


Figure 13. Measured velocity for *Case 2*

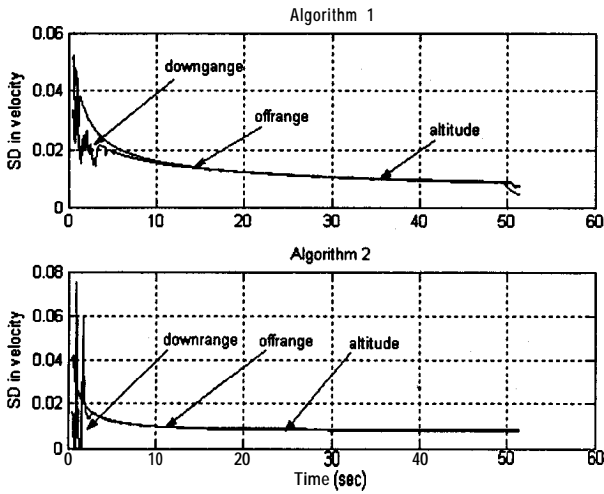


Figure 11. Standard deviation of the estimated velocity for *Case 1*.

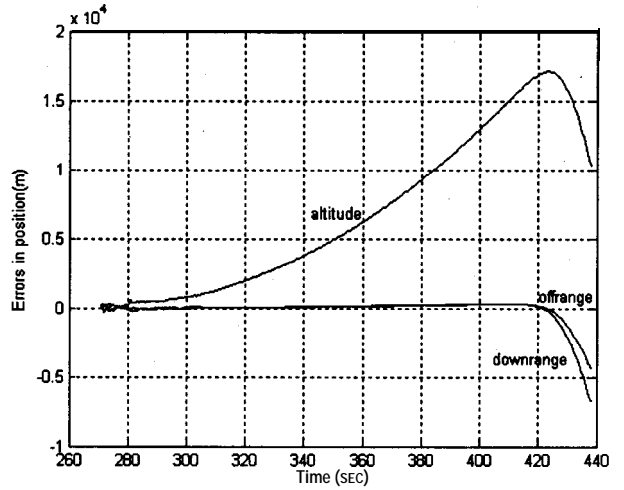


Figure 14. Position estimation error using EKF without input estimation for *Case 2*.

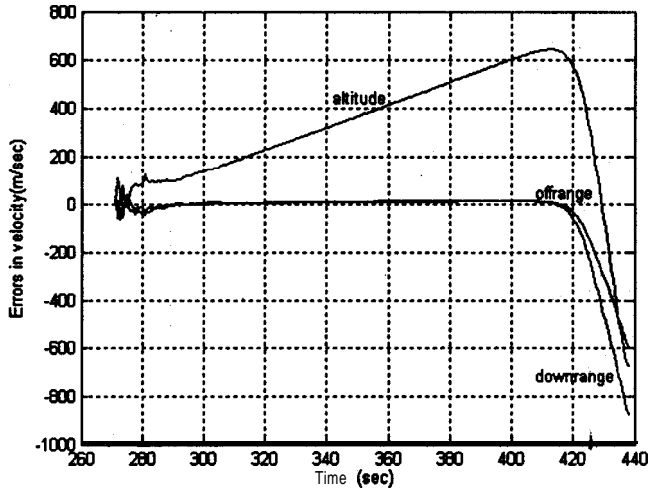


Figure 15. Velocity estimation error using EKF without input estimation for Case 2.

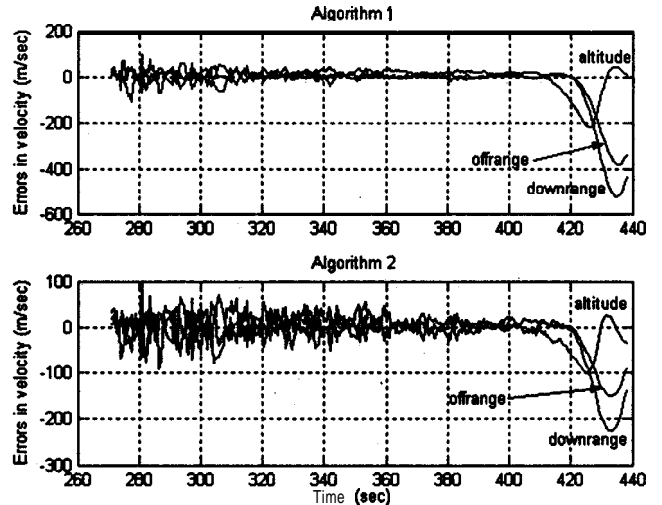


Figure 18. Velocity estimation error using EKF with input estimation for Case 2.

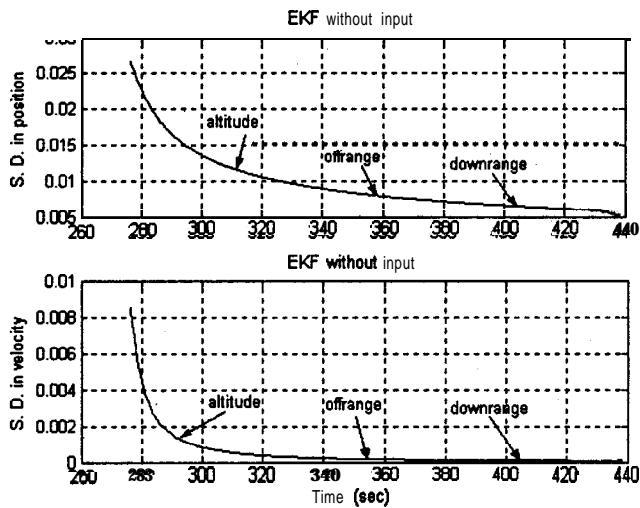


Figure 16. Standard deviation of the estimated states for Case 2.

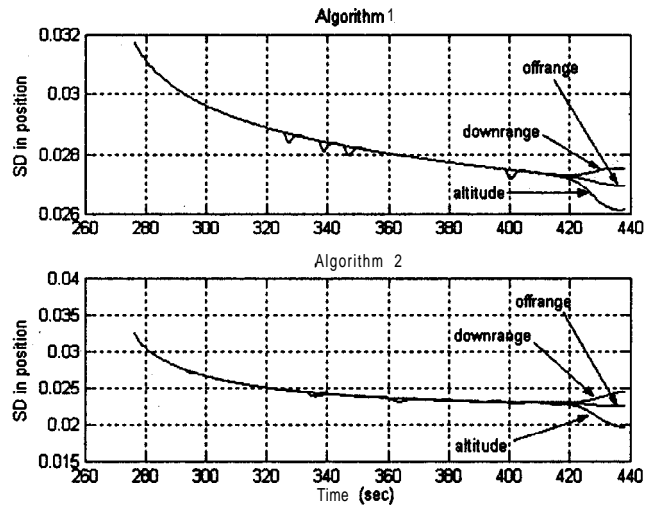


Figure 19. Standard deviation of the estimated position for Case 2.

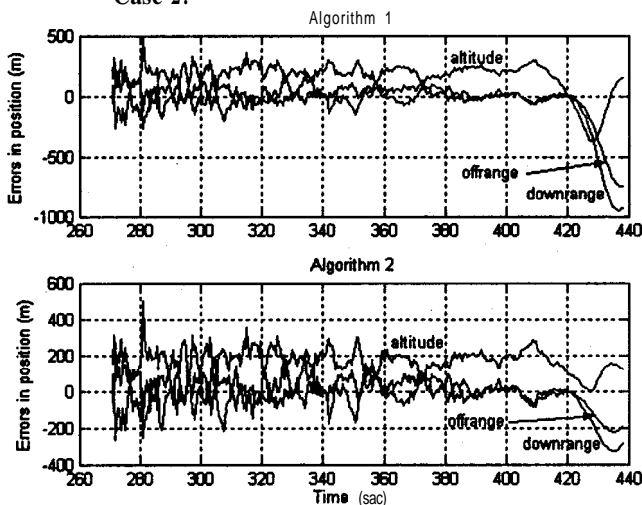


Figure 17. Position estimation error using EKF with input estimation for Case 2.

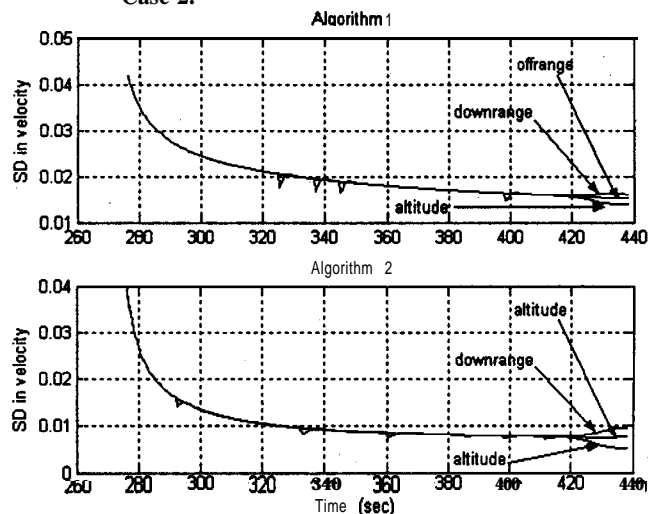


Figure 20. Standard deviation of the estimated velocity for Case 2.

Figures 12 and 13 show the measured trajectory from  $t = 270$  s to  $t = 440$  s, detected by a precision radar. The noises in the measured trajectory are simulated from a noise model of that radar. Let  $C_b = 9646.5 \text{ kg/m}^*$ ,  $\alpha = 0.95$ ,  $R = 0.03 \text{ I}$ ,  $Q = 0.03 \text{ I}$ , and  $\Delta t = 0.5 \text{ s}$ . Initial of  $V$  is taken as  $20 \text{ I}$  too. Figures 14 and 15 show the estimation errors in position and velocity along three axes using the **EKF** with no input and figure 16 displays their standard deviation. The maximum errors of the estimated position and velocity in altitude reach to 17 km and 610 m/s, respectively. It seems too large for **tracking** and intercepting a reentry vehicle. Figures 17 and 18 illustrate the estimation errors using the EKF with two input estimation algorithms.

These are significantly less than using the EKF that the proposed approach is still much better than the **EKF** like the results of Case 1. Input estimation contributes to reduction of error. Furthermore, **algorithm 2 provides a more accurate trajectory estimation** under a **6-DOFs** model which has a large model error. Figures 19 and 20 display the standard deviations of the estimated error induced by the EKF with input estimation. The plots of standard deviation for three methods are consistent for **Case 1**.

### 6. REAL FLIGHT ANALYSIS

A set of real **flight** data is utilised to demonstrate the performance of the two algorithms of input

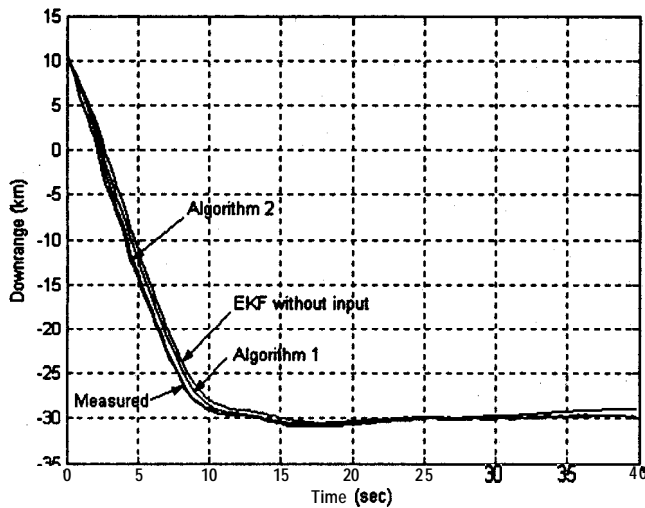


Figure 21. Position estimation in downrange

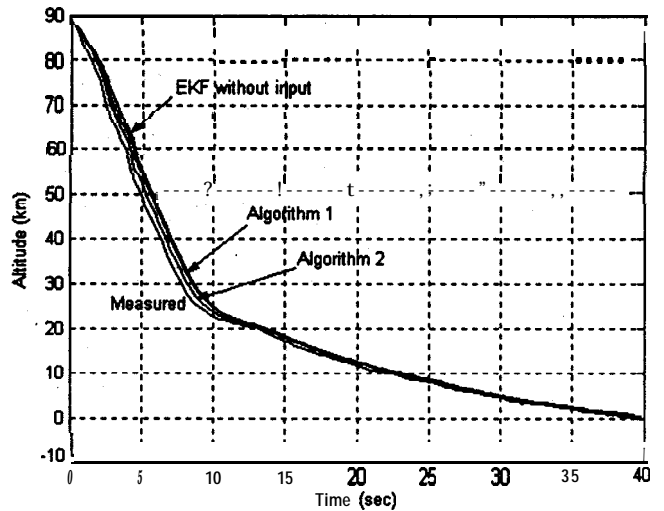


Figure 23. Position estimation in altitude

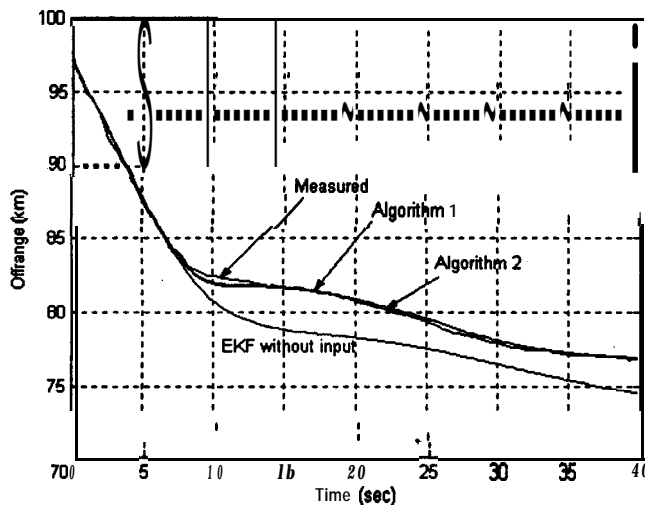


Figure 22. Position estimation in offrange

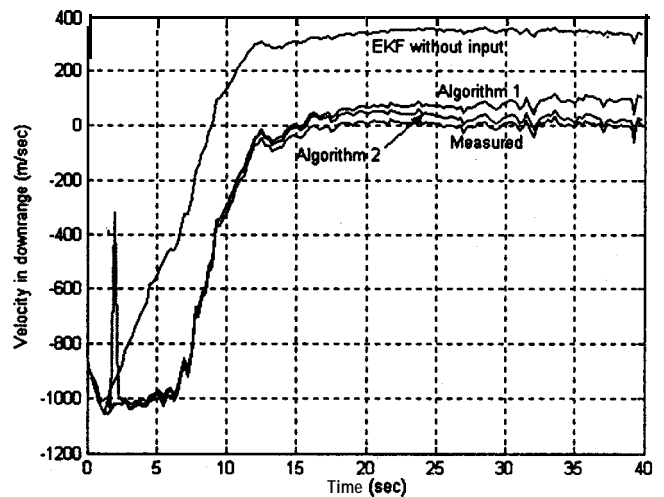


Figure 24. Velocity estimation in downrange

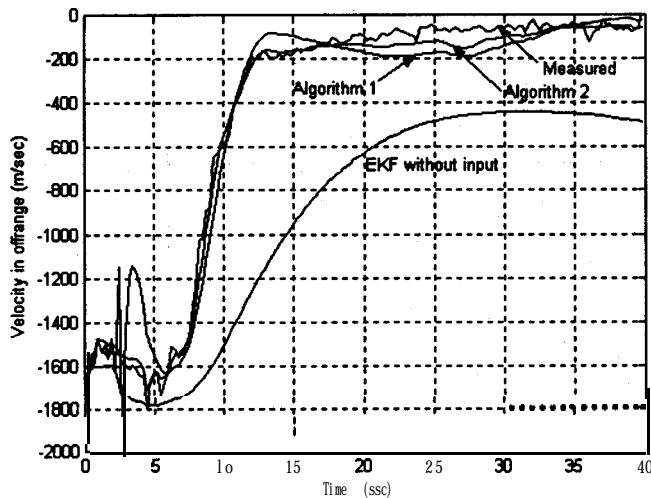


Figure 25. Velocity estimation in offrange

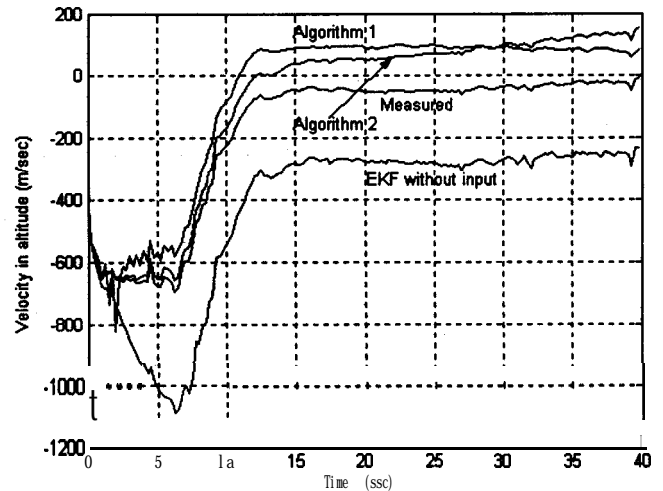


Figure 26. Velocity estimation in altitude

estimation considered. The reentry vehicle was launched at about 400 km from the impact point. The raw measured 40 s data span of the reentry vehicle by a precision radar with sampling rate 4 Hz in this flight test was utilised for this study. The reentry vehicle was first detected by the radar after reentry in the coast phase at a range of 132.5 km with  $\hat{r}_0$   $\hat{\theta}_0$  and  $\hat{\phi}_0$  wrt the radar. Let  $C_b = 9646.5 \text{ kg/m}^2$  during estimation. Figures 21 to 26 show the comparison of the measured and estimated trajectories in downrange, offrange, and altitude, respectively. The filtered trajectories, including position and velocity, using the EKF with input estimation follow the measured trajectory well, as opposed to estimation using the EKF without input estimation. Algorithm 2 provides a trajectory more close to the measured trajectory than algorithm 1. It is consistent with the simulation results.

## 7. CONCLUSIONS

The model error is the main difficulty for trajectory estimation and is solved by the proposed input estimation method. Two recursive algorithms for input estimation under different assumptions about input have been introduced. This investigation presents estimation methods, composed of the extended Kalman filter and two input estimation algorithms, to improve the accuracy of the reentry vehicle trajectory estimation. Algorithm 1 is derived by assuming the input to be constant over operation time of a system. Assumption

of constant input within the sampling period yields algorithm 2, which is more accurate but complicated than algorithm 1. The performance of these two algorithms has been evaluated by simulations, in terms of trajectory estimation errors, and real flight analysis. Algorithm 1 or 2 may be chosen by examining the major concern. The trajectory estimation approach based on algorithm 1 or algorithm 2 is worthy of further study and applications.

## REFERENCES

1. Abutaleb, A.S. Improved trajectory estimation of manoeuvring reentry vehicles using a nonlinear filter based on the Pontryagin minimum principle. *In* IEEE International Radar Conference, Arlington, VA, 1985. pp. 424-29.
2. Lindgren, A.G.; Irz, A. J. & Nardone, S.C. Trajectory estimation with uncertain and nonassociated data. *IEEE Trans. Aerospace & Elect. Syst.*, 1986, AES-22, 71-78.
3. Denis, N.J. Space-based tactical ballistic missile launch parameter estimation. *IEEE Trans. Aerospace & Elect. Syst.*, 1993, AES-29, 412-24.
4. Chu, Q.P.; Mulder, J.A. & van Woerkom, P.T.L.M. Modified recursive maximum likelihood adaptive filter for nonlinear aircraft flight-path reconstruction. *J. Guid. Cont. Dyn.*, 1996, 19, 1285-295.

5. Klein V.; Batterson J.G. & Murphy, P.C. Determination of airplane model structure from flight data by using modified **stepwise** regression. NASA-TP-1916, 1981.
6. Chang, C.B.; Whiting; R.H. & Athans, M. On the state and parameter estimation for maneuvering reentry vehicles. *IEEE Trans. Auto. Cont.*, 1977, AC-22( 1), **99-** 105.
7. Manohar, D.R. & Krishnan, S. Trajectory reconstruction during thrusting phase of rockets using differential corrections. *J. Guid. Cont. Dyn.*, 1985, 8, 406-08.
8. Chan, Y.T. & Hu, A.G.C. A Kalman filter based tracking scheme with input estimation. *IEEE Trans. Aero. Elect. Syst.*, 1979, AES-15, 237-44.
9. Chan, Y.T.; Plant J.B. & Bottomley, J. A Kalman tracker with a simple input estimator. *IEEE Trans. Aero. Elect. Syst.*, 1982, AES-18, 235-41.
10. Bogler, P.L. Tracking a maneuvering target using input estimation. *IEEE Trans. Aero. Elect. Syst.*, 1987, AES-23, 298-10.
11. Tuan, P.C.; Ji, C.C.; Fang, L.W. & Huang, W.T. An input estimation approach to online two-dimensional inverse heat conduction problem. *Num. Heat Trans.*, Part B, 1996, **29**, 345-63.
12. Tuan, P.C. & Fong, L.W. An IMM tracking algorithm with input estimation. *Int. J. Syst. Sci.*, 1996, 27, 629-39.
13. Liu, C.Y.; Lee, S.C. & Hou, W.T. Initial leveling using an adaptive Kalman filter. *J. Chung Cheng Inst. Technol.*, 1997, 25, 147-62.
14. Lee, S.C. & Liu, C.Y. Fast automatic leveling subject to abrupt input. *IEEE Trans. Aero. Elect. Syst.*, 1999, AES-35, 989.
15. Lee, S.C. & Liu, C.Y. Trajectory estimation of reentry vehicles by use of online input estimation. *J. Guid. Cont. Dyn.*, 1999, 22, 808-1 5.
16. Siouris, G.M. Aerospace avionics system: A modern synthesis. Academic Press Inc, 1993. **460p**.
17. Zarchan, P. Tactical and strategic missile guidance, American Institute of Aeronautics and Astronautics Inc, 1994. **pp.** 363.
18. Gelb, A. Applied optimal estimation. *In* The M.I.T. Press, MA, 1974. pp. 107-12.

## Appendix 1

It gives the detailed steps for the proposed extended Kaiman filter with two input algorithms. Assume that the input to be estimated is existing from beginning, that is  $l = 1$ . The detection process will automatically stop inserting the estimated input into the extended Kaiman filter with input if the input is absent. The detailed steps are illustrated as follows:

- Step 1*     Setting initial values and letting  $l = 1, k = 1$ .
- Step 2*     Taking new measurement  $Z_{k+1}$  and estimating states using the extended Kaiman filter with no input.
- Step 3*     Calculating residual from  $\bar{Z}_{k+1} = Z_{k+1} - H\bar{X}_{k+1}$ .

Note that *Step 4* has two parts for different input estimation algorithms.

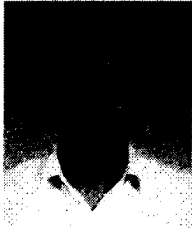
**Algorithm 1**

- Step 4.1*    Calculating  $A$ , from Eqn (19).
- Step 4.2*    Calculating  $B_{k+1}$  From  $B_{k+1} = HA_{k+1} \Phi$ .
- Step 4.3*    Estimating input from Eqn (21).

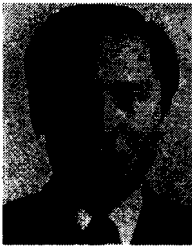
**Algorithm 2**

- Step 4'.1*    Calculating  $\Delta\hat{X}_{k+1-1} = M_{k+1-1} \Delta\hat{X}_{k+1-2} + N_{k+1} \hat{u}_{k+1-2}$ .
- Step 4'.2*    Calculating  $M_{k+1} = (I - K_{k+1}H)\Phi_k$ , and  $N_{k+1} = (I - K_{k+1}H)\Phi$ .
- Step 4'.3*    Calculating  $\Phi_{k+1} = HN_{k+1}$ .
- Step 4'.4*    Calculating the pseudo measurement  $\hat{Y}_{k+1} = \bar{Z}_{k+1} - HM_{k+1} \Delta\hat{X}_{k+1-1}$ .
- Step 4'.5*    Estimating input  $\hat{u}_{k+1-1}$  from Eqn (23).
- Step 5*     Detecting input using Eqn (24). If  $\hat{u}_{k+1-1}$  satisfies Eqn (24), then go to *Step 6*. Otherwise, let  $k = k + 1$  and go back to *Step 2*.
- Step 6*     Estimating states using Eqn (25) and Eqn (26) with the estimated input  $\hat{u}_{k+1-1}$ .
- Step 7*     Letting  $k = k + 1$  and returning to *Step 2*.

## Contributors



**Dr Cheng-Yu Liu** received his MS and **PhD** (Syst Engg) both from the Chung Cheng Institute of Technology, Taiwan, in 1983 and 1998. He had worked at the Chung Shan Institute of Science and Technology from 1985 to 2002. Presently, he is Assistant Professor in the Dept of Electronics Engineering of the Lee-Ming Institute of Technology. His research areas include: System identification, control theory, and tracking system.



**Dr Huai-Min Wang** received his BS (Syst Engg) from the Chung Cheng Institute of Technology, Taiwan, in 1970, MS (**Elec** Engg) from the Standard University at Ann Arbor, USA, in 1979. In 2004, he received his **PhD** (Syst Engg) from the National **Defence** University, Taiwan. He has been working in the Dept of Electrical Engineering of the Fortune Institute of Technology, Taiwan, where he is currently Associate Professor. His major research areas include: Estimation theory, control theory applications, and nonlinear system control.



**Prof Pan-Chio Tuan** received his BS (Syst Engg) from the Chung Cheng Institute of Technology, Taiwan, in 1979, MS (**Mech** and Dynamics) from the Ching Hwa University, Taiwan, in 198 1 and **PhD (Mech)**, from North Carolina State University, USA, in 1991. He has been working in the Dept of Systems Engineering of the Chung Cheng Institute of Technology, Taiwan, since 198 1. Presently, he is Professor. His areas of interest include: Estimation tracking system, and signal processing.